

Geochemistry of Mid Cretaceous Alkaline Volcanic Rocks, member of Chalooos formation, Abbas Abad Volcanic Field, Central Alborz Mountains, North of Iran.

Mohammad Reza Ansari

Faculty of Geoscience Department, Chalooos Branch, Islamic Azad University (IAU), Chalooos, Iran.

*Corresponding Author: m.r.ansari@iauc.ac.ir

Abstract: The Abbas Abad volcanic field (ABVF), North of Iran contains a number of intra-continental alkaline volcanic range situated on central Alborz Mountains, formed along the localized extensional basins developed in relation with the lithospheric thinning and Cretaceous compressional processes. The volcanic suite comprises the extracted melt products of adiabatic decompression melting of the metasomatized mantle that are represented by small-volume intra-continental plate volcanic rocks of alkaline volcanism and their evaluated Rocks with compositions representative of mantle-derived, primary (or near-primary) melts. Trace element patterns with significant enrichment in LILE, HFSE and REEs, relative to Primordial Mantle. Chondrite-normalized of rare earth elements and enrichment in incompatible elements and their element ratios (e.g. Zr/Nb,La/Nb) shown these element modelling indicates that the magmas were generated by comparably variable degrees of partial melting of garnet lherzolite and a heterogeneous asthenospheric mantle source.

[Mohammad Reza Ansari. **Geochemistry of Mid Cretaceous Alkaline Volcanic Rocks, member of Chalooos formation, Abbas Abad Volcanic Field, Central Alborz Mountains, North of Iran.** *Life Sci J* 2013;10(7s):874-883] (ISSN:1097-8135). <http://www.lifesciencesite.com>. 140

Keywords: Abbas Abad area; Iran; garnet lherzolite; partial melting

1. Introduction

Continental volcanic rocks can provide important information about paleo-geodynamic settings and the processes controlling the geochemical evolution of the sub-continental mantle. However, systematic studies of igneous rocks and the chemical composition of the mantle underlying the continental plate are few in number. Alkaline basalt occurs in a variety of geologic and tectonic settings and their detailed study in space and time helps in various ways to understand several geological events. Thought to be an integral part of continental rifting and / or local extensional regime occur in continental fragments. They also serve as major conduits for magma transfer from mantle to the upper crust and constitute a common expression of crustal extension. Another important point is that the continental volcanic rocks have their origin related in some way to the uprise of hot mantle plumes that ultimately may lead to rifting and, ultimately, continental break-up. The mantle source of alkaline basalt is very common and the study of these rocks is an important tool in understanding the evolution of the sub-continental lithosphere and asthenospheric. The magmatic rocks of Alborz mountain range also have different petrological nature. These cretaceous basaltic rocks are well exposed around central part of Alborz mountain ranges, and known as Kojor, Marzan Abad, Amlash, Javherdasht and Javaherdeh Cretaceous volcanic field (GSI, 1997; Haghazar et al., 2009, Ansari et al., 2011), Most previous workers

(GSI, 1997) have given their attention to examine the alkaline rocks only and no petrological and geochemical work is available on these basic rocks. First hand petrological and geochemical information on volcanic rocks of Abbas Abad volcanic field and a suggestion on their possible origin have been resented in the present paper. The detailed petrological and geochemical studies of these rocks are important because most of these follow the direction of major structural features, particularly the deep faults present in the region. Space and time correlation of these rocks with other volcanic rocks suite derived from the sub Alborz mantle plume will help in understanding the continental break-up during the Cretaceous time.

2. Geological setting

The Alborz mountain chain extends for several hundreds of kilometers between the Caspian Sea and the Iranian Plateau (Fig. 1b). The belt is the result of different tectonic events: from the Late Triassic Cimmerian orogeny, resulting from the collision of the Iranian block with Eurasia, to the present day stage of intracontinental deformation related to the convergence between the Arabian and Eurasian plates. Important large-scale features of the belt consist in the lack of an axial metamorphic zone and in the absence of deep crustal roots (crustal thickness is 35 km, according to (Tatar et al., 2002), which is apparently in contrast with the present day elevation of the belt (several summits over 4000 m) which was achieved since Late Miocene (Axen et al.,

2001). The oldest compressional event recorded in the area is the Cimmerian orogeny, which affected the Eurasian margin from Turkey to Thailand. It was chiefly caused by the early Mesozoic collision of several microplates detached from Gondwana. According to palaeogeographic reconstructions (Stocklin, 1974; Stampfli et al., 1991; Saidi et al., 1997; Besse et al., 1998; Stampfli and Borel., 2002) the Iranian microplate was the first block to collide with Eurasia during Middle-Late Triassic forming the Eo-Cimmerian orogen. This event is recorded by a low-angle regional angular unconformity (Stocklin, 1974; Jenny and Stampfli, 1978) along the northern margin of the Iranian plate, sealed by the Upper Triassic-Jurassic Shemshak Formation (Assereto, 1966a; Seyed-Emami, 2003; Fursich et al., 2005). A Permo-Triassic accretionary-subduction complex marking the Paleotethys suture between the Turan and the Iranian plate has been recognized in the Mashad and Torbatjam regions to the east (Ruttner, 1993). Tentatively traces the Paleotethys suture westward across the Gorgan region to the Talesh mountains (western Alborz), where metamorphic napes (Clark et al., 1975; GSI, 1997) are unconformably covered by the Shemshak Formation. The record of the Eo-Cimmerian orogeny is less evident in the central part of the Alborz. The Upper Triassic succession is almost continuous (Ghasemi-Nejad et al., 2004) and is marked by a sudden change in sedimentation, from shallow sea carbonates to siliclastic sandstones, suggesting that central Alborz was located south of the main suture zone and then behaved as a stable foreland region during the collision. The latest Precambrian to Middle Triassic succession is unconformably covered by the Shemshak Formation, up to 4000 m thick, deposited after collision of the Iran microplate to the Eurasian margin. This formation consists of continental sandstones, shale and coal passing upward to shallow marine deposits blanketing the Eo-Cimmerian orogen and its foreland. The shallow water Marine Middle Jurassic–Early Cretaceous carbonates and clastics were followed by early Cretaceous carbonates, basaltic and andesitic volcanic across large parts of the Alborz such as Chaloos formation and Tizkuh formation, which is irregularly preserved and locally folded (Guest et al., 2007). The Abbas Abad middle cretaceous volcanic field is considered a member of Chaloos formation and is located in central part of Alborz mountain ranges. Abbas Abad volcanic alkali rocks is a large composite of the above mentioned volcanic suite which is consist of mainly Olivine basalt-Andesite Basalt (GSI, 1997).

3. Sample Analytic and Method

Nine volcanic rock samples were collected from volcanic outcrops in the Abbas Abad area,

representing the entire mid cretaceous sequence of the central Alborz range. These samples were prepared for analysis major and trace elements and determined by inductively coupled plasma atomic mass spectrometry (ICP-AMS) at ACME lab, Vancouver, Canada, by ANK12000806 and ANK12000803 file number with 4A and 1T-MS full suite packages and shown in Table 1.

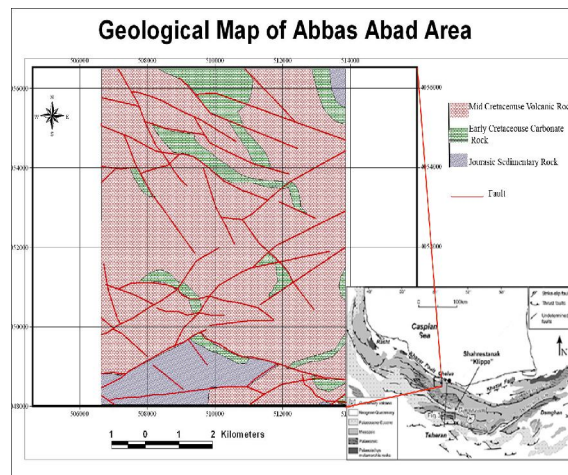


Fig. 1 (a) Simplified geological map of the Abbas Abad area, from GSI.(1997)and our own observations.(b) Tectonic map of the Central Alborz, modified from Allen et al., (2003). (Zanchi et al., 2006).

4. Petrography

The petrography of the Abbas Abad Volcanic rocks Field (ABVF) (Fig. 1a) along with the geology and the contemporaneous volcanic rocks in vary part of central Alborz mountain has been previously described by, (GSI, 1997; Haghazari et al., 2009, Ansari et al., 2011). Most of samples have composition range between olivine Basalt Andesite to olivine Andesite Basalt. An overall consideration of the investigated akalin volcanic rocks indicates that primary mineralogy composed of olivine + plagioclase (Labradorite) + clinopyroxene (augite) ± brown amphibole (xenocryst) ± Phelogopite (xenocryst) + opaque oxides (e.g. Titanomagnetite), whereas the secondary mineral phases are represented by serpentine ± chlorite.

5. Major and Trace Element Geochemistry

The lavas from Abbas Abad basaltic volcanic field (ABVF) are a strongly alkaline series of volcanic rocks, all samples plotting in Shoshonitic series on (K₂O) vs. silica (SiO₂) (Pecceirillo and Taylor, 1976) (Fig. 2) and in the alkali basalt domain on a total alkalis (K₂O+Na₂O) vs. silica (SiO₂) (Le Bas et al., 1986) classification diagram of (Fig. 3).

Table 1: Major (wt %) and trace element (ppm) concentration of chemical composition of the investigated from ABVF alkali volcanic rocks.

	AS9	AS12	AS13	AS14	AS16	AS7	AS8	AS11	AS15
SiO ₂	57.21	37.54	55.69	56.85	55	58.86	57.03	59.08	56.91
Al ₂ O ₃	16.49	11.15	16.71	16.13	15.79	17.01	16.68	16.76	16.52
Fe ₂ O ₃	6.48	13.49	6.72	6.9	6.64	5.92	5.81	5.8	6.37
MgO	2.26	10.87	2.14	2.44	3.89	1.43	2.26	1.72	1.68
CaO	4.16	12.93	3.86	4.3	4.82	3.13	4.3	3.91	3.96
Na ₂ O	4.91	3.06	4.78	4.63	4.45	5.23	5.28	5.19	4.76
K ₂ O	4.12	1.3	3.64	4.28	4.06	4.77	4.1	3.99	3.79
TiO ₂	1.3	2.37	1.19	1.38	1.35	1.25	1.22	1.09	1.27
P ₂ O ₅	0.82	0.95	0.7	0.71	0.74	0.66	0.61	0.57	0.69
MnO	0.07	0.18	0.05	0.07	0.09	0.06	0.08	0.1	0.06
CrO ₃	0.01	0.051	0.006	0.009	0.008	0.007	0.006	0.009	0.007
LOI	1.7	5.5	4.1	1.9	2.7	1.3	2.2	1.4	3.5
Pb	13.50	4.90	12.60	18.77	12.51	15.82	10.26	92.95	7.75
Zn	77.2	114.5	89.2	74.2	72.0	69.2	59.5	75.0	73.5
Ni	50.2	200.5	34.1	50.6	52.3	23.8	23.3	29.1	36.5
Co	23.1	68.2	20.5	25.0	23.0	14.9	16.0	17.1	19.6
Mn	550	1392	384	514	657	412	537	801	452
As	2.8	2.2	3.2	9.3	4.9	4.9	2.2	2.1	2.8
U	4.4	2.9	4.9	5.1	5.2	4.2	3.7	5.6	3.9
Th	21.8	11.2	22.8	29.6	26.8	28.7	29.1	26.6	21.1
Sr	1103	1288	992	1212	1155	1018	1064	1101	1287
Cd	0.16	0.22	0.16	0.16	0.21	0.29	0.20	0.22	0.16
V	58	259	75	72	82	42	51	76	67
La	115.9	79.4	100.6	113.7	108.6	111.7	112.4	98.0	108.0
Cr	63	315	41	61	45	29	24	40	44
Ba	1210	727	1178	1083	1033	1087	1166	1268	1233
Zr	268.2	257.3	315.7	281.1	311.4	371.0	323.4	320.2	216.3
Sn	1.2	2.2	0.5	2.9	1.4	1.5	0.9	1.2	0.4
Be	3	3	4	3	3	3	3	3	3
Sc	6.9	15.5	5.9	7.1	7.3	5.1	4.8	5.7	6.4
Y	13.5	25.6	13.5	15.4	15.3	12.7	13.1	12.1	13.9
Ce	184.51	141.45	163.77	190.76	182.39	178.00	180.58	160.43	179.12
Pr	18.5	16.7	16.7	19.3	18.5	17.7	17.9	15.6	18.1
Nd	56.4	57.7	49.7	61.3	60.7	52.0	56.1	46.6	58.3
Sm	8.0	11.3	7.5	8.5	8.6	6.9	7.6	6.8	8.0
Eu	2.2	3.5	2.2	2.3	2.4	2.3	2.1	1.9	2.4
Gd	4.7	8.5	3.7	4.7	4.3	4.2	3.3	3.9	3.9
Tb	0.6	1.3	0.7	0.7	0.7	0.5	0.6	0.6	0.6
Dy	2.8	5.7	2.9	3.2	3.2	2.8	2.6	2.5	2.8
Ho	0.5	1.1	0.6	0.5	0.6	0.5	0.5	0.4	0.5
Er	1.1	2.2	1.1	1.2	1.2	1.0	1.1	1.0	1.2
Tm	0.2	0.3	0.2	0.2	0.2	0.1	0.2	0.1	0.2
Yb	1.2	1.4	1.0	1.2	1.4	1.1	1.0	0.8	1.1
Lu	0.1	0.2	0.1	0.2	0.2	0.2	0.2	0.1	0.2
Hf	5.79	6.05	6.96	6.53	7.34	8.01	7.46	7.39	4.79
Li	6.9	11.4	4.0	14.2	13.1	9.4	10.0	9.3	10.3
Rb	89.9	20.0	80.8	114.6	97.2	90.2	85.6	86.7	82.3
Ta	4.4	6.1	4.3	4.5	3.6	3.3	5.0	5.0	3.7
Nb	79.51	106.27	74.76	75.08	61.14	47.44	86.23	86.84	59.42
Cs	1.2	0.7	1.3	1.7	1.1	1.0	1.5	1.9	1.6
Ga	21.32	21.62	23.75	22.13	20.54	20.51	23.08	23.72	21.73

The alkaline rocks are mainly, sodic ($\text{Na}_2\text{O}/\text{K}_2\text{O}=1-2.3$) and have low Mg#, and wide range of SiO₂ content from (37.54 to 59 wt. %), Ca (3.13–12.93 wt. % CaO) and Al₂O₃ (11–17 wt. %) contents. Their Cr and Ni concentrations range variably from 24 to 315 ppm and from 23 to 200ppm, respectively. On the Zr/TiO₂ vs. Nb/Y diagram of Winchester and Floyd (1977), the ABVF rocks fall in basanite field, excepted sample AS7, fall into Trachyandesite field (Fig. 4). Although, rock types and whole-rock chemical compositions indicate that they are closer to primary melt compositions the

alkaline rocks have almost straight and relative to chondrite normalized (CN indicates chondrite normalized) REE pattern with near-constant concentration ratios. The ABVF lavas also enriched in LILE, HFSE and REEs (e.g., relative to the Primordial mantle, Primitive mantle normalizing values), that characterize basalts from intraplate continental and/or oceanic island basalt settings. These rocks also display prominent negative Ti, Hf and slightly Ta, Sr anomalies and shown Th, La, Tb, P and Zr positive anomalies. Ocean island basalts (OIBs) (Fig. 6), with strong enrichment in all highly

incompatible elements, shown this enrichment in HFSE, LILE and trace element is upper than 1 and in MREE and HREEs this enrichment is lower than 1. However, shown a positive anomalies in Th, Pb, La, Nd and negative anomalies in Rb, Nb, P and Ti. All samples have REEs enriched patterns on Chondrite-normalized REE plots, the REE show a continuous decrease of normalized concentrations from La to Yb. The REE patterns have extreme slope through the LREE to MREE and HREEs, with (La/Yb) CN ratios of 38.2–82.6, (La/Sm) CN ratios of 4.4–10.2, (Eu/Yb) CN ratios of 4.8–7.1 in the alkali volcanic rocks (Fig. 7).

5.1. TECTONIC SETTING

Meschede (1986) showed that within-plate alkaline basalt and E-MORB could be identified without ambiguity on the triangular plot of Zr–Nb–Y, which is also confirmed by Rollinson, 1993; Dicheng Zhu et al., 2007; Ansari et al., 2011. The Zr–Nb–Y diagrams (Fig. 8) shown the ABVF samples fall near the A1 field, so, illustrate that the ABVF samples are characteristic of within-plate alkaline basalts, which to a large extent resemble the representative OIB (Sun and McDonough, 1989).

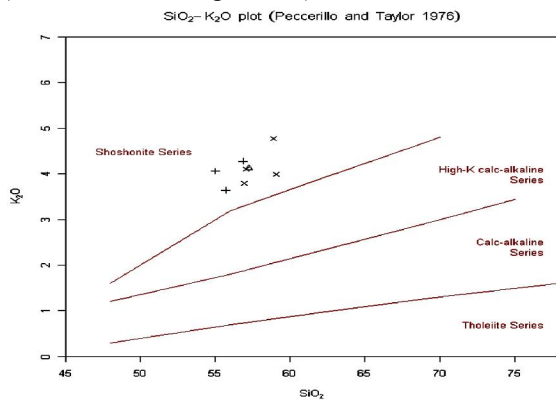


Fig. 2 Classification of the ABVF alkali volcanic rock samples in the (K₂O) vs. silica (SiO₂). (Peccerillo and Taylor, 1976).

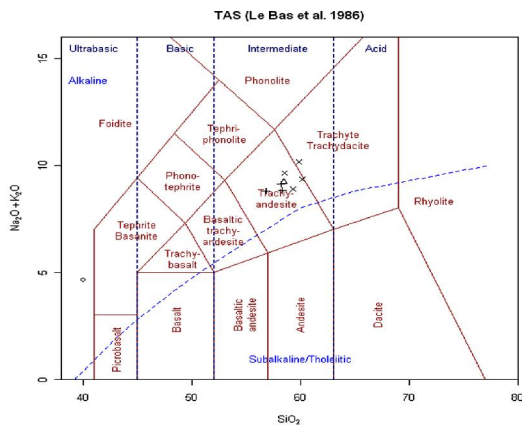


Fig. 3 Classification of the ABVF alkali volcanic rock samples in the TAS diagram after Le Bas et al., (1986) with alkaline/sub-alkaline magma series.

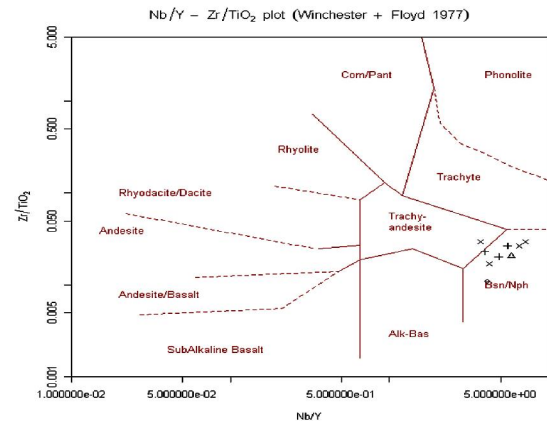


Fig. 4 Nb/Y–Zr/TiO₂ diagram of Winchester and Floyd (1977) showing the alkaline volcanic rock

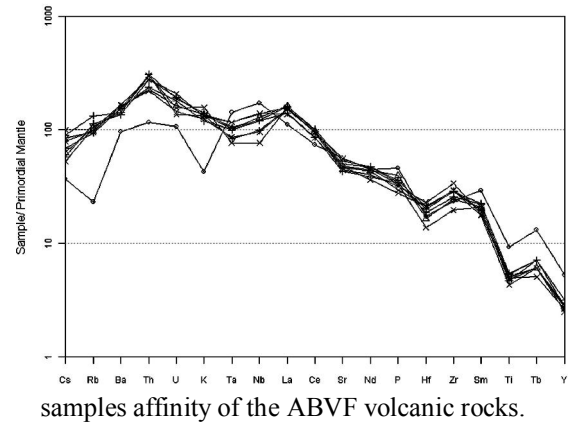


Fig. 5 Primordial mantle-normalized trace element diagrams showing the compositions of ABVF alkali volcanic rocks. Primitive mantle normalizing composition is from (Sun & McDonough, 1989).

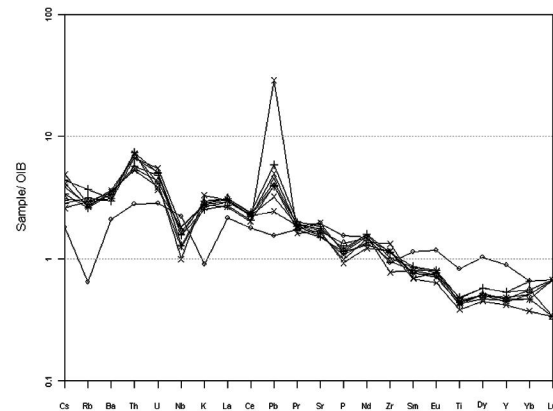


Fig. 6 OIB normalized trace element diagrams showing the compositions of ABVF alkali volcanic rocks. Primitive mantle normalizing composition is from (Sun & McDonough, 1989).

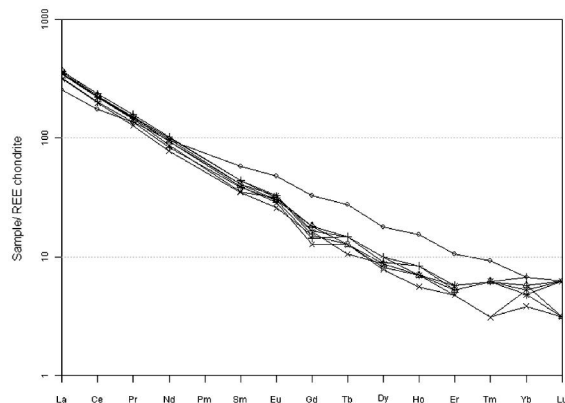


Fig. 7 Chondrite-normalized REE diagrams for ABVF alkali volcanic rocks. Normalizing values are from (Boynnton, 1984)

Generally, basaltic lavas in a continental rift setting are associated with a mantle plume, the asthenosphere, the lithospheric mantle and continental crust (Sun and McDonough, 1989). Therefore, key to study the Petrogenesis of mafic rocks is to identify the relative contributions made by mantle plumes, the normal asthenosphere, the lithospheric mantle and the continental crust (Ansari et al., 2011). Chemical variation of HFSE, HREEs and their ratio such as Zr/Y, Zr/Nb and Y/Nb values are used to identification of mantle and magmatic source/s. The Zr/Y ratios increasing in contrast Zr variation of ABVF rocks, reflected relatively high values owing to higher incompatibility of Zr compared to Y in mantle phases (e.g. Pearce and Norry, 1979; Pearce, 1980; Nicholson and Latin, 1992; Kaan et al., 2009). However, the ABVF rocks could have been generated by varying degrees of melting. It must also be noted that amphibole fractionation may have accounted for a small increase in Zr/Y ratios (Kaan et al., 2009). High Zr/Y values of ABVF samples ($Zr/Y = 10-36.9$) may suggested their derivation from enriched mantle sources or possible contribution of a mantle plume (OIB, $Zr/Y = 9.66$, E-MORB = 3.32; Sun and McDonough, 1989) or derivation from mantle metasomatized and/or by vary degrees of low melting. The Zr/Nb values of ABVF samples ($Zr/Nb = 2.4-7.8$) also support this suggestion. On the other hand, considerable high Zr/Nb values together with relatively low Zr/Y ratios couldn't provide the contribution of depleted mantle during their generation (MORB, $Zr/Y = 2.64$, $Zr/Nb = 31.8$; Sun and McDonough, 1989). Lowest Y/Nb

values ($Y/Nb = 0.1-0.26$) may be related to the involvement of enriched mantle sources and considered the garnet is a present phase in the source. The being of residual garnet results in depletion of HREE relative to LREE because of the strong retention of HREE in garnet (e.g. Wilson, 1989; Spath et al., 1996; Ansari et al., 2011), as also indicated by high partition coefficients of those elements (e.g. Green et al., 1989; Jenner et al., 1994).

The ABVF alkali volcanic rocks display considerable depletion HREE compared to LREE ($[La/Yb]_{CN}$) suggesting the presence of garnet as a residual phase in the source of these rocks, thus, It must also be noted that $[Tb/Yb]_{CN}$ values of ABVF alkali volcanic rocks ($[Tb/Yb]_{CN} = 1.9-3.9$, respectively) are somewhat in agreement with those of alkaline basalts from Hawaii ($[Tb/Yb]_{CN} = 1.89-2.45$), which are also thought to be derived from a garnet-bearing source. However high Dy/Yb ratios displayed by ABVF alkali volcanic rocks ($Dy/Yb = 1.5-2.64$) with respect to that of chondrite ($Dy/Yb = 1.49$; Sun and McDonough, 1989) on the other hand, may suggest a garnet-bearing lherzolite source for the derivation of these alkaline basalts. Taking the geochemical discrimination diagrams into account it is concluded that the ABVF alkali volcanic rocks were formed in a continental extensional setting, although the volcanic rocks have similar geochemical features to OIB.

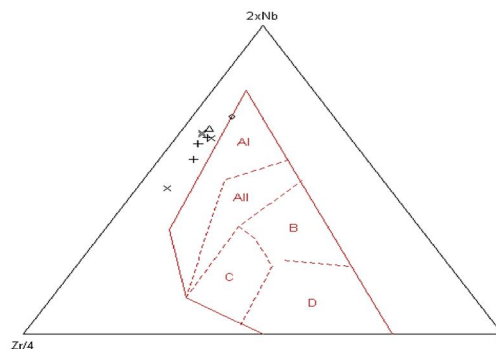


Fig. 8 Nb-Zr-Y discrimination diagram (Meschede, 1986) for the ABVF alkali volcanic rocks. The fields are defined as follows: AI, within-plate alkali basalts; AII, within-plate alkali basalts and within-plate tholeiites; B, E-type MORB; C, within-plate tholeiites and volcanic-arc basalts; D, N-type MORB and volcanic-arc basalts.

5.2. PETROGENESIS OF ALKALINE ROCKS AND MANTEL PROCESS

The foregoing description suggests that the ABVF alkali volcanic rocks may have been derived from mantle source materials resembling those of many oceanic island basalts. This will be further

corroborated in the following discussion. Nb, Th and La are immobile elements and seawater alteration would not change the Nb/Th and La/Nb ratios (Dicheng Zhu et al., 2007). These ratios are also not susceptible to magma processes because they have similar partition coefficient (Li, 1993; Dicheng Zhu et al., 2007; Ansari et al., 2011). The island arc basalts, MORB and OIB can be distinguished well by La/ Nb–La diagram, obviously, the most of ABVF alkali volcanic rock samples plots within the OIB field are shown in the following diagram (Fig. 9). On the other hand, Shaw et al, 2003; Weinstein et al, 2006 argued that alkali basaltic magmas are formed by relatively shallow melting of lithospheric mantle. The $(\text{Sm}/\text{Yb})_{\text{CN}}-(\text{La}/\text{Sm})_{\text{CN}}$ diagram (Fig.10) illustrates the approximate melt compositions of the ABVF alkali volcanic rocks, which fall between the garnet lherzolite field non-modal fractional melting curves, suggesting that the magmas were formed by the melting of garnet lherzolite and we find no evidence for spinel lherzolite melting. The notable fractionation between the LREE, MREE and HREE (high $(\text{La}/\text{Sm})_{\text{CN}}$ (4.4–10.1) and $(\text{Sm}/\text{Yb})_{\text{CN}}$ (6.5–9.1) of the ABVF alkali volcanic rocks correspond a low degree of partial melting of garnet lherzolite. Most of authors (e.g., Mehdizadeh et al., 2002; Liotard et al., 2008; Taki et al., 2009) suggested magmatism in Alborz mountains related to an subduction zone and enrichment event must have modified the mantle source prior to the initiation of partial melting. Metasomatic agents affecting the mantle sources may have included either volatile-rich partial melts or H₂O–CO₂ fluids that originated from the dehydration or partial melting of subducted slabs (Menzies and Hawkesworth, 1987; Hawkesworth et al., 1990) or from plume heads (McKenzie, 1989; Tainton and McKenzie, 1994).

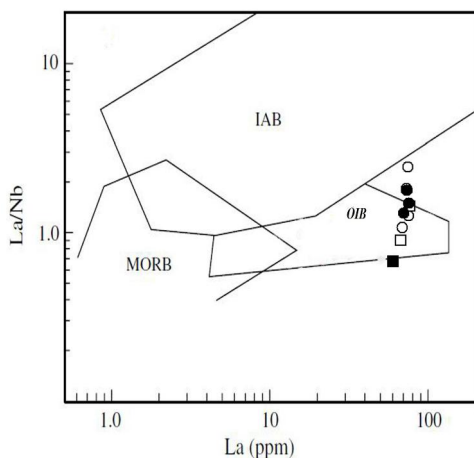


Fig. 9 Trace element discrimination diagrams for the tectonic setting of the ABVF alkali volcanic rocks, North of Iran, La vs La/Nb diagram after (Li, 1993)

showing characteristics of an OIB-type source. The fields are defined as follows: IAB, Island-arc basalts; MORB, mid-ocean ridge basalts; OIB, oceanic island basalts.

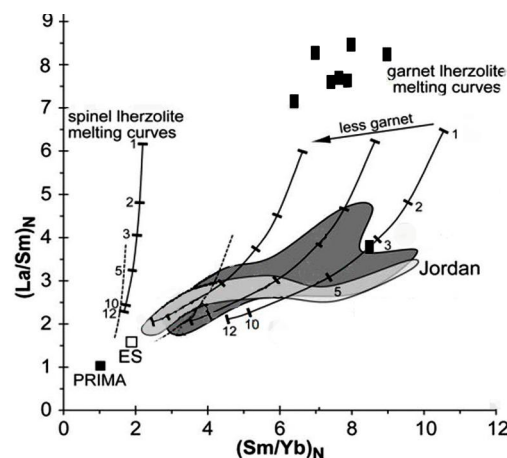


Fig. 10 Diagrams of chondrite-normalized La/Sm vs Sm/Yb for uncontaminated Syrian HAS lavas. Additionally, data fields are from Weinstein et al. (2006); Shaw et al. (2003) for the Israeli and Jordanian HAS lavas, respectively. Also shown are melting curves for non-modal batch melting of garnet and spinel lherzolites of PRIMA compositions (dashed lines) and enriched source compositions (representing mantle enriched with 15% of a 2_5% melt from 0_5% depleted mantle of PRIMA composition) with variable amounts of garnet (continuous lines); the numbers give the degree of melting. PRIMA and chondrite values are from (McDonough & Sun, 1995; McDonough, 1990).

A number of geochemical studies on Damavand dormant volcano and other basaltic rocks in Alborz mountains shown Nb, Ta, and Ti depletions, LILE enrichment, positive Ba and Pb anomaly as well as their similarity to the shoshonitic series lavas were regarded as a ubiquitous subduction zone signature by (Mehdizadeh et al., 2002; Liotard et al., 2008; Taki et al., 2009). These authors also indicated that the enrichment event was related to subduction of either the ocean-like Caspian crust to the southwest or the Paleo-Tethyan subduction, induced by the Zagros formation, to the northeast. Recently published studies suggest, on the contrary, that the northwest extrusion of the South Caspian region was accommodated by subduction beneath the north Caspian region to the north (Axen et al., 2001; Allen et al., 2002; Allen et al., 2003; Ritz et al., 2006; Hollinsworth et al., 2008). In addition, a number of studies on the geodynamic of the Paleo-Tethys demonstrate that Paleo-Tethys oceanic crust subducted northward from Late Devonian to Late Triassic time underneath the Turan Plate. On the

other hand, Jaffarian et al., 2008 and Haghazadeh et al., 2009, mentions, alkali basalt magmatism in central Alborz related to deep mantle melting and/ or mantle plume accompanied by crustal contamination in local extensional regime and/ or deep faults system. Alborz orogenic belt formed by continental-continental collision between the central Iranian block and the Eurasian plate (Vernant et al., 2004), therefore, Alborz region, exhibiting plateau morphology with an elevation 3000-5000 m above sea level. Geophysical studies have revealed that a mantle lithosphere is almost completely absent beneath the Alborz Mountains (e.g., Sodoudi et al., 2009; Mirnejad et al., 2010). Bouguer anomaly Gravity modeling estimated crustal thickness of 35–45 km under the central Alborz and stimulated the idea of root deficiency (Dehghani and Makris, 1984; Amjadi et al., 2012). A relatively thicker crust (45–46 km) was shown for the same region based on surface wave analysis of a few events (Asudeh, 1982; Doloei and Roberts, 2003). The relatively thin crust for a 100 km wide, 3–5 km high mountain range has also been interpreted to be indicating lack of compensation by a lithospheric root (Guest et al., 2007). Inadequate crustal root and the relatively thin lithosphere beneath the Alborz may imply that asthenospheric mantle is supporting the high elevation (Sodoudi et al., 2009). Absence of a crustal root in the Alborz may be due to lower crustal flow and sub-continental delamination as speculated by Allen et al., 2003; Mirnejad et al., 2010. Deep mantle melting and the delamination of sub-continental lithosphere in collision zone are explained by (Lustrino, 2005) and in Central Alborz explained by Ansari et al., 2011. This model presented here is based on the role of lower crust and lithospheric mantle recycling by delamination and detachment. This process can explain at least some geochemical peculiarities of basaltic rocks found in large igneous provinces, as well as in small volume igneous activities, as well as in mid-ocean ridge basalts (Lustrino, 2005). Metamorphic reactions occurring in the lower continental crust as a consequence of continent–continent collision lead to a density increase (up to 3.8 g/cm³), This process leads to gravitative instability of the over thickened lithospheric (lower crust+ lithospheric mantle), so, That lithosphere detached, keel and sink into the Asthenosphere, then upper crust thinning caused by isostasy and thrust/ strike slip faults system, Therefore, Asthenosphere replaced near the upper crust and then beginning various of degree melting.

In summary, major and trace element data, suggest that the ABVF alkali volcanic rocks may have been derived from an OIB-type metasomatized mantle source/s without major affecting of contribution subcontinental lithospheric mantle

and/or lower crust. This study indicated that a huge piece of subcontinental lithospheric mantle (SCLM) and/ or lower crust of beneath Alborz mountain ranges has been delaminated and detached from the upper crust in the past, which caused the thinning of lithosphere by graben structure and continental rifting. In general, isostatic relaxation follows regional shortening and thrust/nappe formation during continent-continent collision. The volume opened by the removal SCLM would be replaced by a new hot asthenospheric mantle plume. Melt and/ or fluid derivation from lower crust or SCLM could be hydrated and metasomatized mantle plume (Lustrino, 2005; Keskin, 2005). Therefore, adiabatic ascent and hydration of asthenospheric mantle cause melt derivation from asthenospheric mantle by decompressing of mantle. The variable degrees of partial melting (Fig. 10) observed in the source of the ABVF lavas are probably due to the pulsing influx of mantle plume material (Krienitz et al., 2007; Ansari et al., 2011).

6. CONCLUSION

This study present new chemical data significant to our understanding of mid cretaceous intraplate magmatism related to sub-continental lithospheric mantle delamination, asthenospheric mantle upwelling, graben structure, deep fault and local rift system in Abbas Abad volcanic suite, central Alborz mountain ranges, North of Iran.

1. The ABVF alkali volcanic rocks have domain rock type between olivine basalt to olivine andesitebasalt.
2. The major minerals composition of the ABVF alkali volcanic rocks are controlled with olivine, plagioclase (Labradorite), clinopyroxene, brown amphibole (xenocryst) ± Phelogopite (xenocryst) + opaque oxides.
3. The major element variation and the REEs variability ratio of ABVF alkali basalts, could be produced by decompressing of a garnet lherzolite metasomatized mantle source/s and vary degrees of partial melting.
4. The chemical and isotopic data shown ABVF alkali volcanic rocks were derived from an OIB-type metasomatized mantle source and are generated from heterogeneous source/s with prominent geochemical heterogeneities.

References

1. Allen MB, Ghassemi MR, Shahrabi M, Qorashi M (2003). Accommodation of late Cenozoic oblique shortening in the Alborz range, northern Iran. *Journal of Structural Geology* 25: 659–672.
2. Allen MB, Jones S, Ismail-Zadeh A, Simmons M, Anderson L (2002). Onset of subduction as

- the cause of rapid Pliocene–Quaternary subsidence in the south Caspian basin. *Geology* 30: 775–778.
3. Amjadi A, Moteshrei A, Theroied SAA, Ansari MR (2012). Estimation of Moho Depth using Bouguer Anomaly Gravity Data. *Innova Ciencia*. Vol4, No7.
 4. Ansari MR, Vossoughi Abedini M, Darvish Zadeh A, Sheikhzakariaee S J, Hossein mirzaee Beni Z (2011). Geochemical Constrains on the Early Cretaceous, OIB-type Alkaline Volcanic Rocks in Kojor Volcanic Field, Central Alborz Mountain, North of Iran. *Australian Journal of Basic and Applied Sciences* 10: 913-925.
 5. Assereto R (1966) a. The Jurassic Shemshak Formation in central Alborz (Iran). *Rivista Italiana di Paleontologia e Stratigrafia* 72: 1133-1182.
 6. Asudeh I (1982). Seismic structure of Iran from surface and body wave data. *Geophysical Journal Royal of Astronomy Society* 71: 715–730.
 7. Axen GH, Lam PS, Grove M, Stokli DF, Hassanzadeh J (2001). Exhumation of the west-central Alborz Mountain, Iran: Caspian subsidence, and collision-related tectonics. *Geology* 29: 559–562.
 8. Besse J, Torcq F, Gallet Y, Ricou L E, Krystyn L, Saidi A (1998). Late Permian to Late Triassic palaeomagnetic data from Iran: constraints on the migration of the Iranian block through the Tethyan Ocean and initial destruction of Pangaea. *Geophysical Journal International* 135, 77e92.
 9. Boynton WV (1984) Geochemistry of the rare earth elements: meteorite studies. In: Henderson P (ed) *Rare earth element geochemistry*. Elsevier, Amsterdam, pp 63–114
 10. Clark GC, Davies RG, Hamzepour G, Jones CR (1975). Explanatory text of the Bandar-e-Pahlavi quadrangle map, 1:250,000. Geological Survey of Iran, Tehran, Iran. pp.198.
 11. Dehghani G, Makris J (1984). The gravity field and crustal structure of Iran. *Neues Jahrbuch für Geologie und Palaeontologie Abhandlungen* 168: 215–229.
 12. Dicheng Zhu A, Guitang Pan A, Xuanxue Mo B, Zhongli Liao A, Xinsheng Jiang A, Liquan Wang A, Zhidan Z (2007). Petrogenesis of volcanic rocks in the Sangxiu Formation, central segment of Tethyan Himalaya: A probable example of plume–lithosphere interaction. *Journal of Asian Earth Sciences* 29: 320–335.
 13. Doloe J, Roberts R (2003). Crust and uppermost mantle structure of Tehran region from analysis of teleseismic P-waveform receiver functions. *Tectonophysics* 364: 115–133.
 14. Fursich FT, Wilmsen M, Seyed-Emami K, Cecca F, Majidifard R (2005). The upper Shemshak Formation (Toarcian–Aalenian) of the Eastern Alborz (Iran): Biota and palaeoenvironments during a transgressive-regressive cycle. *Facies* 51: 365-384.
 15. Geological Survey of Iran (1997). Chaloos Geological Map, scale 1:100,000.
 16. Ghasemi-Nejad E, Agha-Nabati A, Dabiri O (2004). Late Triassic dinoflagellate cysts from the base of the Shemshak Group in north of Alborz Mountains, Iran. *Review of Palaeobotany and Palynology* 132: 207-217.
 17. Green TH, Sie SH, Ryan CG, Cousens DR (1989). Proton microprobe determined partitioning of Nb, Ta, Zr, Sr and Y between garnet, clinopyroxene and basaltic magma at high pressure and temperature. *Chem Geol* 74: 201–216
 18. Guest B, Guest A, Axen F (2007). Late Tertiary tectonic evolution of northern Iran: a case for simple crustal folding. *Global and Planetary Change* 58: 435–453.
 19. Haghazadeh Sh, Vossoughi Abedini M, Poor Moafi M (2009). Petrology and Geochemistry of Mafic Rock in Javaher Dasht area, East of Gillan Province, North of Iran. PhD thesis in Shahid Beheshti University, 298pp.
 20. Hawkesworth CJ, Kempton PD, Rogers NW, Ellam RM, Calsteren P, Giggenbach W (1990). Continental mantle lithosphere, and shallow level enrichment processes in the Earth's mantle. *Earth and Planetary Science Letters* 96: 256–268.
 21. Hollingsworth J, Jackson J, Walker R, Nazar H (2008). Extrusion tectonics and subduction in the eastern South Caspian region since 10 Ma. *Geology* 36: 763–766.
 22. Jaffarian A, Emami H, Vossoughi Abedini M, Ghaderi M (2009). Petrology and Geochemistry of Lower Paleozoic Magmatism in the East of Alborz. PhD thesis in IAUS, 298pp.
 23. Jenner GA, Foley SF, Jackson SE, Green TH, Fryer BJ, Longerich H P (1994). Determination of partition coefficients for trace elements in high pressure–temperature experimental run products by laser ablation microprobe-inductively coupled plasma mass spectrometry (LAM-ICP-MS). *Geochim Cosmochim Acta* 58: 5099–5130.
 24. Jenny J, Stampfli G (1978). Lithostratigraphie du Permien de l'Elbourz oriental en Iran. *Eclogae geologicae Helveticae* 71: 551-580.
 25. Kaan SM, Cema G (2009). Geochemistry of mafic rocks of the Karakaya complex, Turkey: evidence for plume-involvement in the Palaeotethyan extensional regime during the

- Middle and Late Triassic. *Int J Earth Sci* 98: 367- 385.
26. Keskin M (2005). Domal uplift and volcanism in a collision zone without a mantle plume: evidence from eastern Anatolia. *MantlePlume.Org*
 27. Krienitz MS, Hasse KM, Mezger K, Shaikh-Mashail MA (2007). Magma genesis and mantle dynamic at the Harrat Ash Shaam volcanic field (South Syria). *JOURNAL OF PETROLOGY* 48: 1513-1542.
 28. Le Bas MJ, Le Maitre RW, Streckeisen A, Zanettin BA (1986). Chemical classification of volcanic rocks based on the total alkali-silica diagram. *J Petrol* 27:745–750
 29. Li SG (1993). Ba–Nb–Th–La diagrams used to identify tectonic environments of ophiolite. *Acta Petrologica Sinica* 9: 146–157 (in Chinese with English abstract).
 30. Liotard JM, Dautria JM, Bisch D, Condomines J, Mehdizadeh H, Ritz JF (2008). Origin of the absarokite–banakite association of the Damavand volcano (Iran): trace elements and Sr, Nd, Pb isotope constraints. *International Journal of Earth Sciences* 97: 89–102.
 31. Lustrino M (2005). How the Delamination and Detachment of Lower Crust Can Influence Basaltic Magmatism. *Earth-Science Reviews*.
 32. McDonough WF, Sun SS (1995). The composition of the Earth *Chemical Geology* 120: 223–253.
 33. McDonough WF (1990). Constraints on the composition of the continental lithospheric mantle. *Earth and Planetary Science Letters* 101: 1–18.
 34. McKenzie D (1989). Some remarks on the movement of small melt fractions in the mantle. *Earth and Planetary Science Letters* 95: 53–72.
 35. Mehdizadeh H, Liotard JM, Dautri JM (2002). Geochemical characteristics of an intracontinental shoshonitic association: the example of the Damavand volcano, Iran. *Comptes Rendus Geoscience* 334, 111–117.
 36. Menzies MA, Hawkesworth CJ (1987). *Mantle Metasomatism*. Academic Press, London.
 37. Meschede M (1986). A method of discriminating between different type of mid-ocean ridge basalts and continental tholeiites with the Nb–Zr–Y diagram. *Chemical Geology* 56: 207–218.
 38. Mirnejad H, Hassanzadeh J, Cousens BL, Taylor BE (2010). Geochemical evidence for deep mantle melting and lithospheric delamination as the origin of the inland Damavand volcanic rocks of northern Iran. *Journal of Volcanology and Geothermal Research*, 198: 288-296.
 39. Nicholson H, Latin D (1992). Olivine tholeiites from Krafla, Iceland: evidence for variation in melt fraction within a plume. *J Petrol* 33:1105–1124.
 40. Pearce JA (1980). REE values for various OIB etc, From lead isotope study of young volcanic rocks mid-oceanic ridges, oceanic islands and island arcs. *Philos Trans R Soc Lond A* 297: 409–445.
 41. Pearce JA, Norry M (1979). Petrogenetic implications of Ti, Zr, Y and Nb variations in volcanic rocks. *Contrib Mineral Petrol* 69: 33–47.
 42. Ritz JF, Nazar H, Ghasemi A, Salamati R, Shafei A, Solaymani S, Vernant P (2006). Active transtension inside central Alborz: a new insight into northern Iran–southern Caspian geodynamics. *Geology* 34: 477–480.
 43. Rollinson, HR (1993). *Using Geochemical Data: Evaluation, Presentation, Interpretation*. Longman, New York, p. 352.
 44. Rudnick RL, Gao S (2003). The composition of the continental crust. In: Rudnick, R.L. (Ed.), *The Crust*. In: Holland, H.D., Turekian, K.K. (Eds.), *Treatise on Geochemistry*, vol. 3. Elsevier, Oxford, pp. 1–64.
 45. Ruttner AW (1993). Southern borderland of Triassic Laurasia in north-east Iran. *Geologische Rundschau* 82: 110-120.
 46. Saidi A, Brunet MF, Ricou LE (1997). Continental accretion of the Iran Block to Eurasia as seen from Late Palaeozoic to early Cretaceous subsidence curves. *Geodynamica Acta* 10, 189e208.
 47. Seyed-Emami K (2003). Triassic in Iran. *Facies* 48, 95e106. Sengor, A.M.C., 1984. The Cimmeride orogenic system and the tectonics of Eurasia. *Geological Society of America Special Publication* 195: 82 pp.
 48. Shaw J (2003). *Geochemistry of Cenozoic volcanism and Arabian lithospheric mantle in Jordan*. Ph.D. thesis, Royal Holloway University of London, 268 pp.
 49. Sodoudi F, Yuan X, Kind R, Heit B, Sadidkhoy A (2009). Evidence for a missing crustal root and a thin lithosphere beneath the Central Alborz by receiver function studies. *Geophysics Journal International* 177: 733–742.
 50. Spath A, Le Roex AP, Duncan RA (1996). The geochemistry of lavas from the Comores Archipelago, Western Indian Ocean: petrogenesis and mantle source region characteristics. *J Petrol* 37: 961–991.
 51. Stampfli G, Marcoux J, Baud A (1991). Tethyan margins in space and time. *Palaeogeography, Palaeoclimatology and Palaeoecology*.

52. Stampfli GM, Borel GD (2002). A plate tectonic model for the Palaeozoic and Mesozoic constrained by dynamic plate boundaries and restored synthetic oceanic isochrones. *Earth Planetary Sciences Letters* 196: 17-33.
53. Stocklin J (1974). Possible ancient continental margins in Iran. In: Burk, C.A., Drake, C.L. (Eds.), *The Geology of Continental Margins*. Springer, Berlin, pp. 873-887.
54. Sun SS, McDonough WF (1989). Chemical and isotopic systematics of oceanic basalts: implications for mantle composition and processes. In: Saunders AD, Norry MJ (eds) *Magmatism in the ocean basins*. *Geol Soc Spec Publ* 42: 313-345
55. Tainton KM, McKenzie D (1994). The generation of kimberlites, lamproites and their source rocks. *Journal of Petrology* 35: 787-817.
56. Taki S, Darvishzadeh A, Ghaderi M (2009). *Petrology of Igneous Rocks in Deylaman Area, Central Alborz*. PhD thesis in IAUS, 272pp.
57. Tatar M, Hatzfeld D, Martinod J, Walpersdorf A, Ghafari-Ashtiany M, Chery J (2002). The present-day deformation of the central Zagros from GPS measurements. *Geophysical Research Letters* 29.
58. Vernant P, Nilforoushan F, Chery J, Bayer R, Djamour Y, Masson F, Nankali H, Ritz J F, Sedigh M, Tavakoli F (2004). Deciphering oblique shortening of central Alborz in Iran using geodetic data. *Earth and Planetary Science Letters* 223: 177-185.
59. Weinstein Y, Navon O, Altherr R, Stein M (2006). The Role of Lithospheric Mantle Heterogeneity in the Generation of Plio-Pleistocene Alkali Basaltic Suites from NW Harrat Ash Shaam (Israel). *JOURNAL OF PETROLOGY* 47: 1017-1050.
60. Weinstein Y, Navon O, Lang B (1994). Fractionation of Pleistocene alkali-basalts from the northern Golan Heights, Israel. *Israel Journal of Earth Sciences* 43: 63-79.
61. Wilson M (1989). *Igneous Petrogenesis. A Global Tectonic Approach*. Chapman and Hall, UK.
62. Winchester JA, Floyd PA (1977). Geochemical discrimination of different magma series and their differentiation products using immobile elements. *Chemical Geology* 20: 325-342.
63. Xiao L, Xu YG, Mei H J, Zheng YF, He B, Pirajno F (2004). Distinct mantle sources of low-Ti and high-Ti basalts from the western Emeishan large igneous province, SW China: implications for plume lithosphere interaction. *Earth and Planetary Science Letters* 228: 525-546.
64. Zanchi A, Berra F, Mattei M, Ghassemi M R, Sabouri J (2006). Inversion tectonics in central Alborz, Iran. *Journal of Structural Geology* 28: 2023-2037.
65. Zhu DC, Pan GT, Mo XX, Wang LQ, Liao ZL, Jiang XS, Geng QR (2005). SHRIMP U-Pb zircon dating for the dacite of the Sangxiu formation in the central segment of Tethyan Himalaya and its implications. *Chinese Science Bulletin* 50: 563-568.

2/25/2013